Vol. 561: 123–136, 2016
doi: 10.3354/meps11913

MARINE ECOLOGY PROGRESS SERIES
Mar Ecol Prog Ser

Published December 15

Hydrodynamic effects of macrophyte microtopography: spatial consequences of interspecific benthic transitions

M. Lara[1,*], T. J. Bouma[2], G. Peralta[1], J. van Soelen[2], J. L. Pérez-Lloréns[1]

[1]Department of Biology, Faculty of Marine and Environmental Sciences, University of Cadiz, Campus of International Excellence (CEIMAR), 11510 Puerto Real (Cadiz), Spain
[2]Royal Netherlands Institute for Sea Research (NIOZ-Yerseke), PO Box 140, 4400 AC Yerseke, The Netherlands

ABSTRACT: Rhizophytic green algae of the genus *Caulerpa* are potential competitors with seagrass-dominated habitats. At Cadiz Bay Natural Park, *Caulerpa prolifera* and the seagrass *Cymodocea nodosa* co-occur in overlapping patches, which may be considered as transition zones. In these zones, changes in microtopography are stepped because patches of *C. prolifera* normally occur at 5 to 10 cm above the adjacent *C. nodosa* patches. We hypothesized that hydrodynamics influenced by this microtopography may foster sedimentation on the *C. nodosa* side, which in turn would facilitate the spreading of *C. prolifera*. To test this hypothesis, an experiment simulating the flow between both species was conducted in a race-track flume tank, allowing us to study the influence of unidirectional free stream velocity (low velocity, LV = 0.065 m s^{-1}, vs. high velocity, HV = 0.14 m s^{-1}) and microtopography (flat bottom, FB, vs. stepped bottom, SB) on shear stress (τ), turbulent kinetic energy above the canopy (TKE_{above}) and volumetric flow rate through the canopy (Q_c). Under our experimental conditions, comparison of τ-values with theoretical thresholds revealed sedimentation scenarios. However, at HV, the probability of sedimentation was higher in *C. nodosa* than in *C. prolifera* patches. Moreover, Q_c was higher within *C. nodosa* canopies than within *C. prolifera*, ensuring a higher source of sediment with potential to be trapped within the canopy. Although we found no species-specific differences in TKE_{above} values, they increased with HV increasing the vertical mixing. Overall, conditions for sedimentation seemed more facilitated in *C. nodosa* than in *C. prolifera* in SB only under HV conditions.

KEY WORDS: *Caulerpa prolifera* · *Cymodocea nodosa* · Hydrodynamics · Microtopography · Rhizophytes · Seagrasses

INTRODUCTION

Seagrass meadows are in decline worldwide (Orth et al. 2006), creating opportunities for invasive species, both exotic and native, to occupy these habitats (Occhipinti-Ambrogi & Savini 2003, Williams 2007, Pérez-Ruzafa et al. 2012). Green rhizophytic algae of the genus *Caulerpa* are potential competitors for seagrass-dominated habitats, since seagrass cover is negatively correlated with *Caulerpa* expansions, as reported for both Mediterranean (Bulleri et al. 2010, Hoffman 2014, Pérez-Lloréns et al. 2014) and Atlantic coasts (Stafford & Bell 2006, Tuya et al. 2013a).

The spreading of *Caulerpa* can be grouped in 2 strategies: (1) fragmentation (Ceccherelli & Cinelli 1999, Smith & Walters 1999) and (2) space pre-emption via clonal growth (e.g. Stafford & Bell 2006, Wright & Davis 2006). As a spreading mechanism, the efficiency of clonal expansion is fostered by high levels of sedimentation, which in turn increase the chance for successful colonization (Stafford & Bell

*Corresponding author: miguel.lararayo@uca.es

2006). Episodes of strong sedimentation, increased organic matter and sulphide pools confer competitive advantages to *Caulerpa* species, which grow more efficiently than seagrasses under these conditions (Piazzi et al. 2005, 2007, Holmer et al. 2009, Pérez-Ruzafa et al. 2012).

Species-specific differences in sediment-trapping capacity generally drive changes in water–sediment interactions resulting in depositional gradients along transition zones (TZs) of overlapping macrophyte populations (Gacia et al. 2003, Hendriks et al. 2010). Hendriks et al. (2010) reported that homogeneous canopies of *Caulerpa prolifera* Forsskål (Lamouroux) trapped sediment 2.5 times faster than homogeneous canopies of the seagrasses *Posidonia oceanica* (L.) Delile and *Cymodocea nodosa* Ucria (Ascherson). This high sediment-trapping capacity of *C. prolifera* was attributed to the enhanced vertical transport of particles into the canopy instead of the horizontal transport resulting from advection typical of seagrass beds. In contrast, homogeneous seagrass meadows generally stabilize and retain sediment by reducing water velocity within the canopy (i.e. horizontal processes; Almasi et al. 1987, Gacia et al. 1999, Hendriks et al. 2010). Besides these studies, hydrodynamic gradients within overlapping *Caulerpa* spp. and seagrass patches have only been described in a single *in situ* study (Morris et al. 2013), which reported higher canopy flow permeability in *C. nodosa* than in *C. prolifera* beds. Excepting this latter work, most of the previous studies were conducted *ex situ* and on homogeneous beds with no explanation of the functioning of macrophyte TZs.

However, improving our knowledge of TZ function can be especially relevant for management of macrophyte-dominated coastal habitats, like those at Cadiz Bay Natural Park (CBNP), Spain. Cadiz Bay is a shallow tide-dominated embayment protected from oceanic waves but sporadically affected by wind waves that generate erosive events, mainly under strong easterlies and westerlies (Alvarez et al. 2003). Subtidal vegetated bottoms are mostly represented by the green rhizophyte *Caulerpa prolifera* and the seagrass *Cymodocea nodosa*. Populations of both species occur in a wide belt around the bay and their patches usually overlap at their edges (Morris et al. 2009, 2013, De los Santos et al. 2013). Preliminary data suggested that, under a positive sedimentation scenario (i.e. high sediment load), *C. prolifera* might outcompete *C. nodosa* because (1) *C. prolifera* possesses a lower light compensation point for photosynthesis than *C. nodosa*, which confers a competitive advantage in turbid environments (Pérez & Romero 1992, Vergara et al. 2012) and (2) the biomass turnover rate is also higher for *C. prolifera* than for *C. nodosa* (Brun et al. 2006, Vergara et al. 2012, Olivé et al. 2013), which suggests a better potential for rapid expansion. At CBNP, well-developed TZs between these 2 species usually exhibit a clear microtopographic pattern: the bottom of *C. prolifera* beds is 0.05 to 0.20 m above the adjacent *C. nodosa* stands (Morris et al. 2013, M. Lara pers. obs.). This 'step' extends horizontally between 0.05 and 0.15 m (M. Lara pers. obs.). Although it has been recently described that ripples can be formed in intertidal mudflats under very specific situations, the formation of muddy ripples seems rather improbable at CBNP since these steps do not show any regular spatial pattern (Chang & Flemming 2013). At CBNP, these steps are only evident at the edges of the overlying patches of both species, where *C. prolifera* patches are always found at higher elevations than *C. nodosa* patches.

The effects of microtopography on interactions between macrophyte species have rarely been addressed. Earlier studies dealt with the influence of raising the seagrass bottom on current velocity (Fonseca et al. 1983), the role of microtopography on flow over turf algae (Carpenter & Williams 1993) and the effects of mudflat structure on bed friction (Whitehouse et al. 2000). These studies showed that (1) microtopography enhances bottom shear stress in elevated areas, but it also fosters sedimentation on the adjacent depressed bottom, and that (2) water flow diverges and lessens downstream of the raised bottom. Additionally, it has been reported that the interaction between microtopography and sedimentation may affect macrophytobenthos abundance (Irving & Connell 2002) but also that macrophytes may change the structure of bed form patterns (Marani et al. 2004, Borsje et al. 2009, Bouma et al. 2013). All of these studies highlight that understanding the mechanisms underlying the distribution of benthic habitats requires a better knowledge of the interactions among flow, microtopography and vegetation at TZs.

Here we hypothesized that bottom microtopography affects the hydrodynamics, which ultimately may control the local sediment dynamics in overlapping *C. nodosa* and *C. prolifera* patches. Consequently, the probability of sediment deposition may increase at the TZs between these species, favouring the spread of *C. prolifera*. To test this hypothesis, we conducted a flume-tank experiment to study the combined effects of free stream velocity and bottom microtopography on hydrodynamic variables in simulated adjacent patches of *C. nodosa* and *C. pro-*

lifera. The likelihood of these hydrodynamic measurements to result in potential sedimentation or erodability was evaluated by comparison with theoretical thresholds.

MATERIALS AND METHODS

Plant collection

Caulerpa prolifera and *Cymodocea nodosa* specimens were collected in May 2008 from the inner bay at CBNP, SW Spain (36° 28′ 13″ N, 06° 15′ 7″ W). Several days prior to the experiment, plants were collected, cleaned, wrapped in moist tissue paper and sent to the laboratory at the Royal Netherlands Institute for Sea Research in Yerseke, The Netherlands (NIOZ-Yerseke). Upon arrival, plants were kept in a tank with filtered, aerated seawater (salinity 31, temperature 18°C) under a 14 h light:10 h dark photoperiod with 160 µmol photons m^{-2} s^{-1}. Before each experimental run, plants were checked to replace any damaged specimens with intact ones.

Experimental design and spatial arrangement of patches

Ten siliceous sediment boxes (0.390 × 0.285 × 0.150 m each) were assembled to construct a 2 m long bed within the test section of the flume tank. Each box was planted either with *C. prolifera* or *C. nodosa* specimens. Stolons of *C. prolifera* and rhizomes of *C. nodosa* were buried, ensuring that fronds and shoots remained aboveground. Plant density, leaf length and leaf area index were similar to summer observations at CBNP (Table 1; Vergara et al. 2012, Morris et al. 2013). Regardless of the bottom microtopography level, *C. prolifera* was always placed at the upstream portion of the test section (designated the CP section in Fig. 1; x = 0.8 m, y = 0.6 m), whereas the downstream end was shared by adjacent *C. nodosa* (CN, x = 1.2 m, y = +0.3 m) and *C. prolifera* (x = 1.2 m, y = −0.3 m) beds.

We used a 10 m^3 unidirectional flow flume tank with a 0.6 × 2 m test section and race-track architecture that prevents undesirable secondary flows along the width of the test section (Jonsson et al. 2006, Bal

Table 1. Demographic variables of *Caulerpa prolifera* (CP) and *Cymodocea nodosa* (CN) corresponding to our flume experiment and to literature values described for this species at Cadiz Bay Natural Park (CBNP), Spain, during summer conditions, when wind storms have the highest probability of occurring. Error values indicate 95% confidence intervals

	Plant density (shoots m^{-2})		Leaf length (cm)		Leaf area index	
	CP	CN	CP	CN	CP	CN
Flume expt.	6890	443	4.70 ± 1.33	20.35 ± 9.16	3.66	0.78
CBNP	6500 ± 2150[a] 8700 ± 464[b]	356 ± 190[b]	10.00 ± 2.77[b]	30.00 ± 12.27[b]	4[a]	1.9[b]

[a]Vergara et al. (2012); [b]Morris et al. (2013)

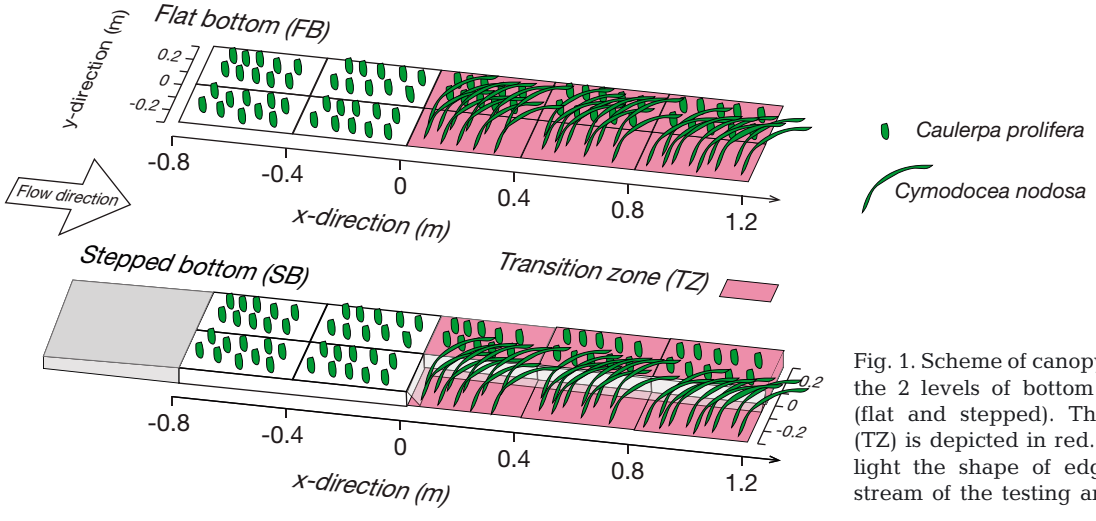

Fig. 1. Scheme of canopy configuration for the 2 levels of bottom microtopography (flat and stepped). The transition zone (TZ) is depicted in red. Grey areas highlight the shape of edge conditions upstream of the testing area and in the TZ

et al. 2013). A preliminary test with a bare bed (free stream velocity ~0.25 m s^{-1}) confirmed minimum differences (0–3%) on *u*-velocity between the left and the right side of the flume (Fig. 2), and hence the effect of artificial secondary flows within complex bed configurations could be disregarded. To avoid any artificial high turbulence intensity by forcing the flow to pass through the canopy bed, a bare space was simulated in between the canopy and the closest wall. Additionally, to keep the hydrodynamic properties of the patches, the water column depth:canopy height ratio was always maintained above 2 (i.e. water column height between 0.32 and 0.42 m, cf. Fonseca & Koehl 2006). This design allows for upscaling to the shallow depths where the overlapping patches of *C. prolifera* and *C. nodosa* normally occur (i.e. –0.5 m in the lowest astronomical tide, Vergara et al. 2012).

To study the effects of microtopography, 2 experimental levels were assayed: flat bottom (FB) and stepped bottom (SB). To simulate the SB, boxes with *C. prolifera* were placed 0.1 m higher than the *C. nodosa* ones (Fig. 1). To avoid undesired effects due to sharp vertical edges formed at the beginning of the TZ (x = 0 m), a smooth 3 m slope (incline = 3%) was simulated upstream of the test section (grey area at the left side of SB, Fig. 1). For a similar reason, the steps on the TZ were also smoothed by adding fine gravel to the slopes. The effects of the fine gravel on the roughness scale of the flume tank were negligible, as the estimation of the granular roughness length (z_0) following Dade et al. (2001) showed the same order of magnitude for bed sediment and for the fine gravel.

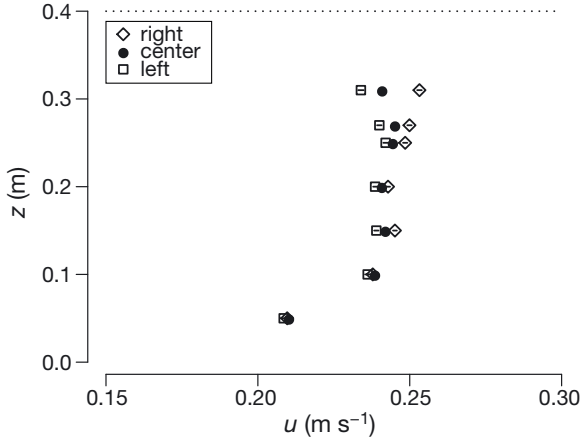

Fig. 2. Vertical profiles of the *u* component of velocity (m s^{-1}) over bare bed areas (control tests). The tests were run at a free stream velocity of 0.25 m s^{-1} and a water column height of 0.4 m (dotted line). The profiles were measured at right (y = 0.05 m), centre (y = 0.00 m) and left (y = –0.05 m) positions within the flume tank. Error bars within the symbols represent the 95% confidence intervals

Each level of microtopography was exposed to 2 levels of unidirectional free stream velocities: low velocity (LV = 0.065 m s^{-1}) and high velocity (HV = 0.14 m s^{-1}). Both levels are representative of the environmental conditions in CBNP. The LV is within the range of typical tidal currents (Morris et al. 2013), whereas the HV is within the maximum current values predicted for CBNP (Kagan et al. 2003). Although we are aware of the likely orbital flow effects, we decided to focus only on unidirectional currents, which are the prevailing currents at CBNP, leaving the effects of waves for further studies.

The 3 velocity components (u, v and w) were measured with an acoustic Doppler velocimeter (ADV, Nortek) set at 10 Hz. Measurements lasted 270 s per sampling point, following a 3-D grid with 280 points in total. The points were distributed over 7 x-locations (–0.15, –0.05, 0.1, 0.15, 0.30, 0.60 and 0.90 m from the leading edge of the TZ), 4 y-locations (–0.20, –0.10, 0.10 and 0.20 m from the centre of the flume tank cross section) and 10 z-locations (0.01, 0.02, 0.03, 0.04, 0.06, 0.08, 0.10, 0.15,0. 20 and 0.24 m above the bottom of the *C. prolifera* bed; 0.03, 0.04, 0.06, 0.08, 0.10, 0.12, 0.15, 0.18, 0.20 and 0.24 m above the bottom of the *C. nodosa* bed). For the SB microtopography, we added 0.10 m to the 3-D grid z locations above the *C. prolifera* bed. To minimize disturbances within the ADV probe (i.e. interaction with the canopy as the probe moves toward the bed), the robotic probe started measurements from its lowest position on each vertical profile. The height of the *C. nodosa* canopy (h_c) was measured at every x-position by drawing the projected area, whereas h_c was relatively constant for *C. prolifera* (~0.04 m). To depict the projected area of canopy, plastic slides were placed on the transparent wall of the flume tank and its upper limit was carefully traced as a thin curve stroke.

Hydrodynamic variables

Prior to data analysis, raw data with beam correlations below 70% were filtered out (Bouma et al. 2007, Lara et al. 2012), leaving at least 2000 data points per 3-D grid measurement point. Once filtered, the velocity components were estimated as time-averaged values ($\bar{u}$, $\bar{v}$, $\bar{w}$) and their respective fluctuation terms (u', v', w'). The turbulent kinetic energy (TKE = 0.5 × [$\overline{u'^2}$ + $\overline{v'^2}$ + $\overline{w'^2}$]) was estimated with values measured close to the top (TKE_{above}) of both *C. prolifera* (~0.04 m) and *C. nodosa* (~0.08–0.18 m) canopies. In this way, TKE_{above} estimated

the magnitude of vertical mixing into the canopy (Hendriks et al. 2010).

The bottom shear stress (τ, Pa; Eq. 1 below) is generally used as a proxy for bed stability and for probability of sedimentation (Fonseca & Fischer 1986, Zong & Nepf 2010). In our case, it was used to compare spatial patterns of sedimentation probability between *C. prolifera* and *C. nodosa* beds. The values of τ were estimated for the range of 0.03 to 0.04 m from the bottom using the near-bed Reynolds stress:

$$\tau = -\rho\overline{u'w'} \quad (1)$$

where τ is bottom shear stress (Pa), ρ is water density (1025 kg m^{-3}), and $\overline{u'w'}$ is the vertical transfer of longitudinal momentum fluctuations (m^2 s^{-2}). This range of elevations (0.03–0.04 m) was chosen for comparative purposes according to the lowest elevation where we could obtain reliable data for *C. nodosa* beds (Hendriks et al. 2010).

To determine the effects of *C. prolifera* and *C. nodosa* on bed stability and sedimentation probability, gradients of τ were analysed according to downstream (x) directions and compared with theoretical thresholds for erosion (τ_{er}) and sedimentation (τ_{sed}). To calculate these thresholds, values of sediment size and composition were assumed to be equal to those previously published for clay (illite: diameter, $d \approx 4$ µm; particle density, ρ_s = 2800 kg m^{-3}), silt (illite: $d \approx 44$ µm; ρ_s = 2800 kg m^{-3}) and fine-sand fractions (quartz, $d \approx$ 280 µm, ρ_s = 2600 kg m^{-3}) at CBNP (Gutierrez-Mas et al. 1997, Achab & Gutierrez-Mas 2005).

The values of τ_{er} were estimated from standardized curves modified from Shield's diagrams (Eqs. 2 & 3), depending on a characteristic dimension of particle size (D^*, Eq. 4; van Rijn 2007):

$$\tau_{er} = 0.115(D^*)^{-0.5}; \text{ for } D^* < 4 \quad (2)$$

$$\tau_{er} = 0.14(D^*)^{-0.64}; \text{ for } 4 \le D^* < 10 \quad (3)$$

$$D^* = d\left(\left(\frac{\rho_s}{\rho_w}-1\right)\frac{g}{v^2}\right)^{\frac{1}{3}} \quad (4)$$

where d is a representative diameter of a particle, ρ_s (kg m^{-3}) is the particle density, ρ_w is the seawater density (1025 kg m^{-3}), g is the gravitational acceleration (m s^{-2}), and v is the kinematic viscosity of water at 15°C (1.15×10^{-6} m^2 s^{-1}).

The values of τ_{sed} were calculated using the empirical relationship reported by Self et al. (1989) (Eq. 5):

$$\log_{10}(\tau_{sed}) = 0.76 \times \log_{10}(d) - 2.76 \quad (5)$$

Finally, the canopy volumetric flow rate (Q_c, m^3 s^{-1}) was a proxy of the effects of factors on the horizontal supply of suspended sediment (Peralta et al. 2008). The values of Q_c were estimated as follows: (1) TZ (i.e. 1.2 m on the test section) was divided into 4 equal sections (i.e. 1.2 m length × 0.15 m width, $y_{1/4W}$ in Eq. 6); (2) the velocity profiles were horizontally integrated rendering Q_i values for each z-layer in each section (Eq. 6); and (3) Q_c was finally estimated as the vertical integration of Q_i within the canopy (Eq. 7). Additionally, the volumetric flow rate above the canopy (Q_{above}) was estimated following a similar procedure (Eq. 8).

$$Q_i = \sum_{j=1}^{j=2} y_{\frac{1}{4}W} \times (z_i - z_{i-1}) \times u_{z_i y_j} \quad (6)$$

$$Q_c = \sum_{0}^{h_c} Q_i \quad (7)$$

$$Q_{above} = \sum_{h_c}^{h_w} Q_i \quad (8)$$

where h_c is the canopy height (m), h_w is the water column height (m), $y_{1/4W}$ is the quarter part of flume tank width and $u_{z_i y_j}$ is the u (m s^{-1}) at height z_i on the corresponding $y_{1/4W}$ and cross-stream positions y_1 and y_2, respectively. The flow rate through the flume tank side corresponding to each species equals to Q_c + Q_{above}. To facilitate the comparison between treatments, Q_c and Q_{above} were normalized by the total flow rate through the entire flume-tank section (i.e. $Q = Q_{cn\_side} + Q_{cp\_side}$), and the resulting values were expressed as percentages (i.e. $\%Q_c$, $\%Q_{above}$).

Statistical analysis

The racetrack flume always yielded n = 8 samples per experimental run (i.e. from 4 x-positions by 2 y-positions) for each species. To discard sample position effects, the relationship between position (covariate) and the corresponding dependent variable was checked for significance using an ANCOVA (Sokal & Rohlf 1995). Accordingly, the effects of sample position on TKE_{above} (F = 1.30, p = 0.25) and τ (F = 0.06, p = 0.8) were negligible compared to the variance due to experimental treatments.

After position effects were disregarded, normality and homoscedasticity requests were checked using Shapiro-Wilks and Levene tests, respectively. To achieve these assumptions, values of τ and TKE_{above} were log-transformed. Following data transformation, the effects of velocity and microtopography were tested with a 2-way ANOVA. The contribution (percentage) of each factor to the total variance was estimated as the sum of squares among treatments (SS).

Finally, 95% confidence intervals (CI) were obtained by spatially averaging the values of $\%Q_c$ or τ. Mean differences were contrasted with the root-sum-of-squared 95% CI to ensure significance ($\alpha = 0.05$).

RESULTS

Velocity profiles

The *u*-profiles revealed species-specific patterns in the vertical flow structure and in efficiency of velocity reduction near the floor (Fig. 3). Regardless of the treatment, velocity values near the bottom were lower within the taller *Cymodocea nodosa* canopy ($u < 0.003$ m s^{-1}) than within the shorter *Caulerpa prolifera* canopy ($u > 0.005$ m s^{-1}). Inter-specific differences in canopy architecture (i.e. height and morphology) could account for the recorded differences in vertical *u*-profile shapes.

In the LV-FB treatment, *u*-velocity decreased shortly after entering the *C. nodosa* canopy (Fig. 3C, $x = 0.1$ m); however, in the HV-FB treatment, such a decrease was detected farther within the canopy (Fig. 3G, $x = 0.3$–0.4 m). Regardless of the velocity level, the SB microtopography favoured the generation of LV regions near the floor of the *C. nodosa* canopy (Fig. 3D,H; $x = 0.1$–0.5 m). Within this depressed region (~0.4 m downstream of the step below the *C. prolifera* bed), the values of velocity measured within the step were 1 order of magnitude lower than those of the FB.

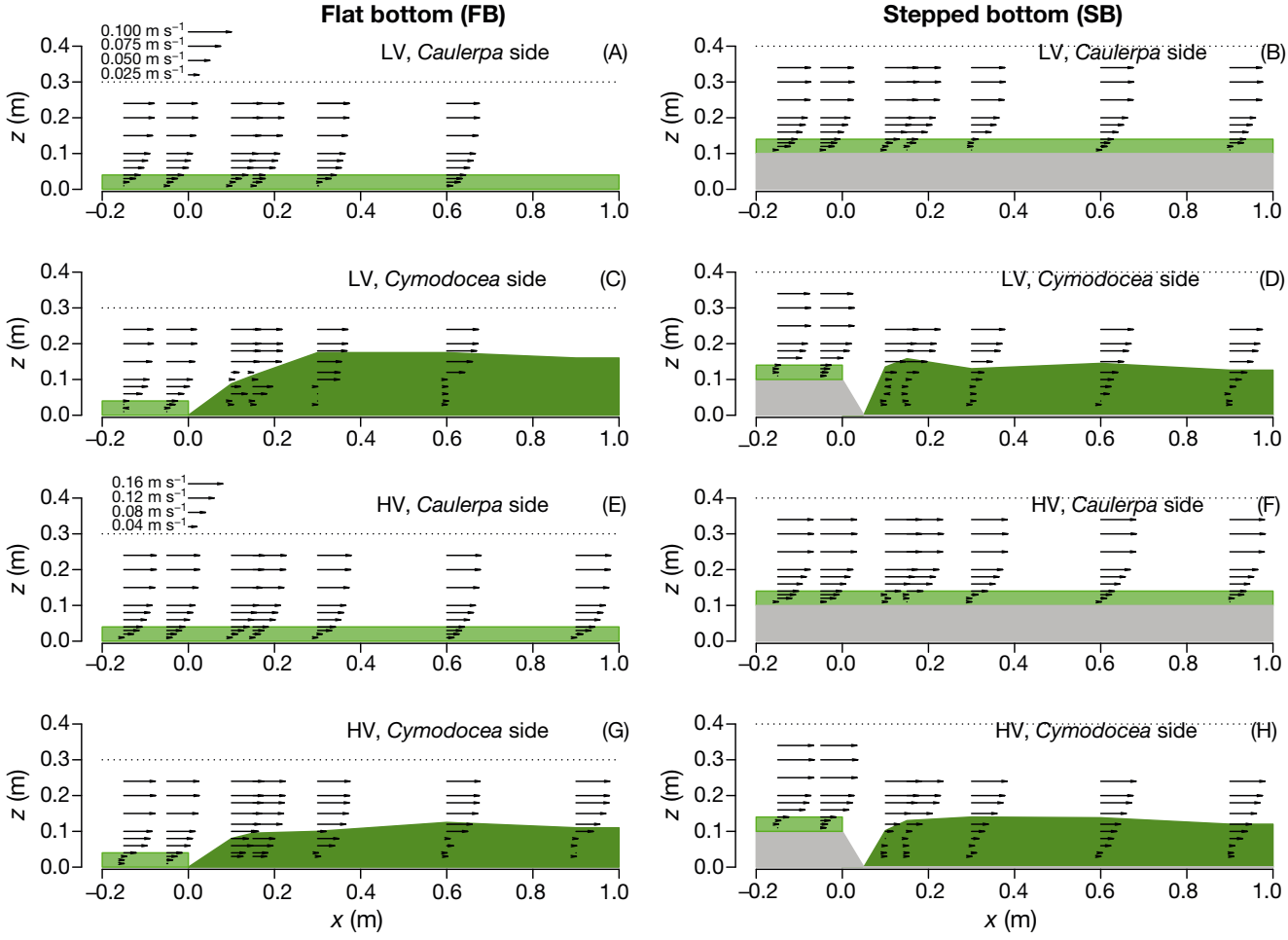

Fig. 3. Vertical profiles of the *u*-component of velocity (m s^{-1}) along the test section (*x*) of the racetrack flume according to the free stream velocity (A–D: low velocity, LV = 0.065 m s^{-1}; E–H: high velocity, HV = 0.14 m s^{-1}) and bottom microtopography (flat or stepped bottom). The *u*-profiles are represented by arrows with lengths proportional to the *u*-values (note that the proportions of the arrows are different at LV and HV). The profiles correspond to *y*-position = 0.1 m for *Caulerpa prolifera* and –0.1 m for *Cymodocea nodosa*. Dotted lines represent the water column height. *C. nodosa* canopies are represented by dark green polygons, *C. prolifera* canopies are light green rectangles, and the bottom microtopography is symbolized by grey polygons

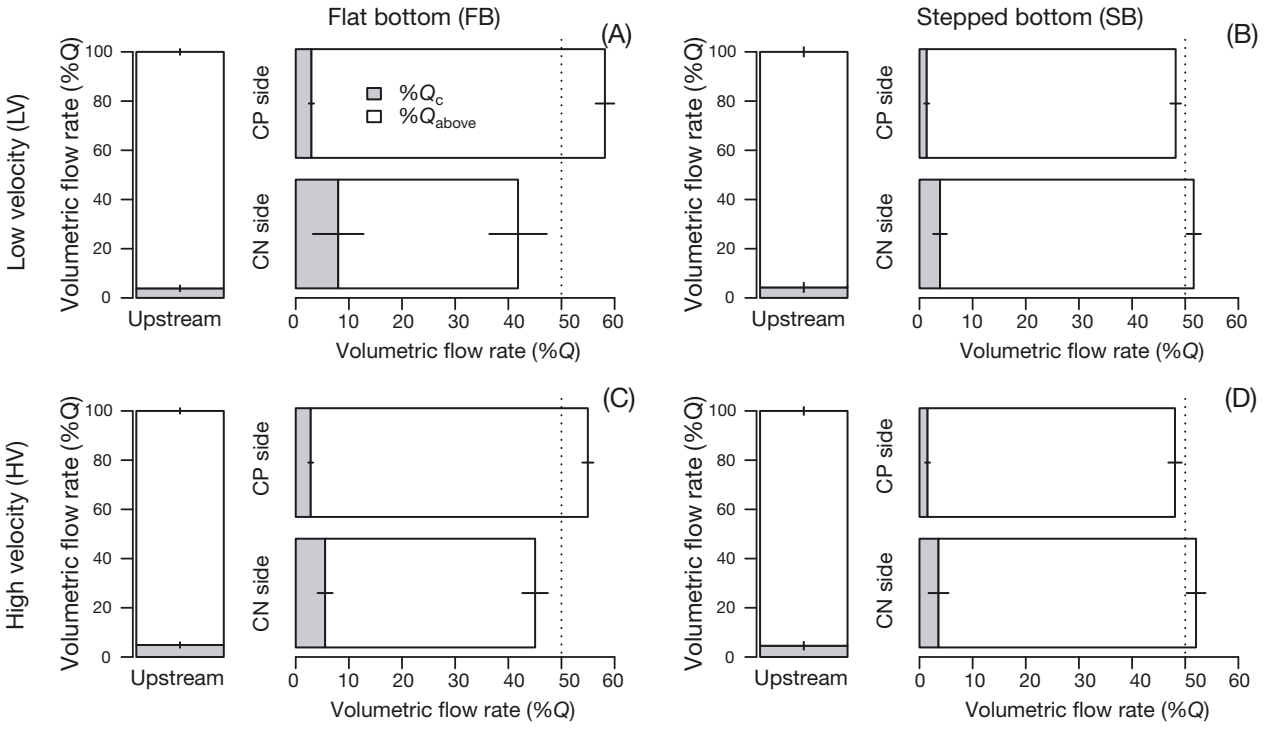

Fig. 4. Volumetric flow rates in the transition zone (TZ), according to the free stream velocity (A,B: low velocity, LV; vs C,D: high velocity, HV) and bottom microtopography (A,C: flat bottom, FB; vs B,D stepped bottom, SB). Data are expressed as percentages of the total volumetric flow rate (Q), which varied at LV between 0.010 (FB) and 0.012 $m^3 s^{-1}$ (SB), and at HV between 0.023 (FB) and 0.027 $m^3 s^{-1}$ (SB). Results are depicted as accumulated bars of $\%Q_c$ (volumetric flow rate crossing the canopies, grey columns) and $\%Q_{above}$ (volumetric flow rate crossing the water above the canopies, white columns). Results on the test section were split in 3 areas: 'Upstream' ($\%Q$ before the TZ, where *Caulerpa prolifera* occupies the entire test section); 'CN side' ($\%Q$ on the TZ side occupied by *Cymodocea nodosa*); and 'CP side' ($\%Q$ on the TZ side occupied by *Caulerpa prolifera*; see Fig. 1 for further details). For TZ areas, the 50% Q is highlighted with a dashed line. Error bars represent 95% confidence intervals

Volumetric flow rates and canopy heights

The volumetric flow rates through each type of canopy were normalized for the total flow crossing the whole flume section ($\%Q_c$) and yielded values below 10% in both species (Fig. 4; grey areas). In contrast, the percentages of volumetric flow rate above each canopy ($\%Q_{above}$) ranged between 30 and 55% of the whole flume section (Fig. 4). Regardless of the experimental treatment, $\%Q_c$ values within *C. nodosa* were generally higher (3.5–8%) than those recorded within *C. prolifera* (1.7–3.2%, non-overlapping 95% CI). Canopy height (h_c) seemed to account for these differences since it was always higher for *C. nodosa* (0.175 m at LV, 0.08 m at HV) than for *C. prolifera* (0.04 m; see Fig. 3 for canopy height details).

For FB microtopography, although $\%Q_c$ was lower in *C. prolifera*, the volumetric flow rate crossing along the side of the flume tank occupied by *C. prolifera* (58% at LV, 55% at HV; Table 2) was always

Table 2. Volumetric flow rates in the transition zone (TZ), according to the free stream velocity (LV: low velocity, HV: high velocity) and microtopography treatments (FB: flat bottom; SB: stepped bottom). Data are expressed as percentages of total volumetric flow rate (Q) and have been separated as percentage of Q crossing the canopies of *Caulerpa prolifera* (CP) and *Cymodocea nodosa* (CN) ($\%Q_c$), and the percentage of Q above those canopies ($\%Q_{above}$). The percentage of Q crossing each side (i.e. $\%Q_c + \%Q_{above}$) is also indicated

Velocity ($m s^{-1}$)	Microtopography and Q ($m^3 s^{-1}$)	Flume side (species)	$\%Q$	$\%Q_c$	$\%Q_{above}$
LV: 0.065	FB (0.0105)	CP	58.2	3.2	55
		CN	41.8	8	33.8
	SB (0.0123)	CP	48.4	1.7	47.1
		CN	51.2	4.4	46.8
HV: 0.14	FB (0.0233)	CP	54.9	3.1	51.8
		CN	45.1	5.5	39.6
	SB (0.0272)	CP	48.4	1.8	46.6
		CN	51.6	3.5	48.1

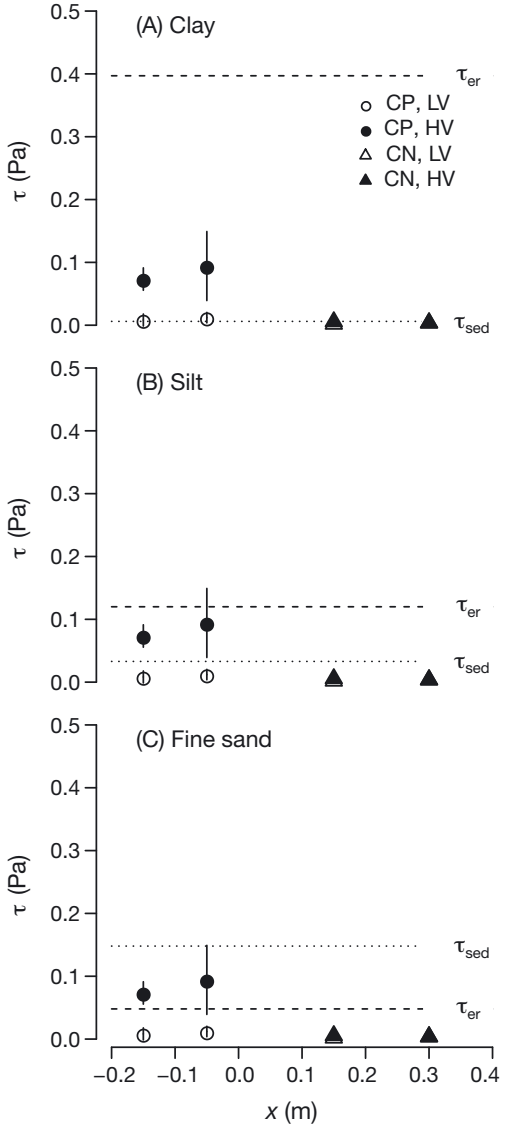

Fig. 5. Comparison of bed shear stress (τ, Pa) with thresholds for erosion (τ_{er}) and sedimentation (τ_{sed}). Thresholds were modelled for (A) clay (diameter, $d \approx 4$ µm; particle density, $\rho_s = 2800$ kg m^{-3}), (B) silt ($d \approx 44$ µm, $\rho_s = 2800$ kg m^{-3}) and (C) fine sand ($d \approx 280$ µm, $\rho_s = 2600$ kg m^{-3}) particles. Since the bottom microtopography had no significant effects on τ, only the results for stepped bottom (SB) are shown. LV: low velocity; HV: high velocity; CP: *Caulerpa prolifera*; CN: *Cymodocea nodosa*

higher than that crossing along the *C. nodosa* side (42% at LV, 45% at HV), clearly indicating that the water flow was preferentially redirected towards the top of the *C. prolifera* bed (non-overlapping 95% CI; Fig. 4A,C). However, these differences were not recorded for SB microtopography, where $\%Q_c$ was practically reduced by half in both species and the volumetric flow was similar for both sides (Fig. 4B,D). Given that the increase in free stream velocity resulted in a proportional enhancement of the total volumetric flow rate ($Q = 0.012$ m^3 s^{-1} for LV versus $Q = 0.027$ m^3 s^{-1} for HV), it counterbalanced the reduction of $\%Q_c$ due to the SB microtopography.

Bottom shear stress (τ)

Free stream velocity significantly affected bed shear stress on *C. prolifera* substrate (circles in Fig. 5, Table 3, $F = 4.422$, $p < 0.05$) but not on *C. nodosa* substrate (triangles in Fig. 5, $F = 4.415$, $p > 0.05$), suggesting that the seagrass has a higher capacity than the rhizophyte in buffering bed instability under unidirectional flow dominated systems. However, SB did not affect the values of τ on any of the 2 vegetated bottoms (Table 3, $p > 0.05$), suggesting that spatial gradients in τ were mainly due to the change in canopy properties rather than to the presence of SB microtopography.

To identify likely consequences for erodability/sedimentation probability, τ values for different grain sizes found at CBNP (i.e. clay, silt and fine sand) were compared with theoretical thresholds for erosion and sedimentation (τ_{er} and τ_{sed}, respectively; Fig. 5). The graphic representation of these thresholds generated 3 possible scenarios: (1) high probability of particle

Table 3. Statistical effects of free stream velocity and microtopography treatments on bed shear stress (τ). Level of significance α = 0.05; n = 8; SS: sum of squares; MS: mean squares

Factor	df	SS	MS	*F*	% SS	p
(A) *Caulerpa prolifera* (n = 8)						
Free stream velocity	1	8.55	8.55	4.422	10	0.046
Microtopography	1	6.19	6.19	3.201	14	0.086
Free stream velocity × Microtopography	1	0.13	0.13	0.065	–	0.800
Residuals	24	46.40	1.933			
(B) *Cymodocea nodosa* (n = 8)						
Free stream velocity	1	20.87	20.87	4.415	–	0.050
Microtopography	1	0.04	0.04	0.008	–	0.931
Free stream velocity × Microtopography	1	8.61	8.61	1.821	–	0.195
Residuals	17	80.35	4.727			

erosion ($\tau \geq \tau_{er}$); (2) high probability of sedimentation ($\tau_{sed} > \tau$); and (3) an intermediate state in which the particles remain in suspension ($\tau_{er} > \tau > \tau_{sed}$). For fine sand, the τ threshold for sedimentation was higher than for erosion ($\tau_{sed} > \tau_{er}$), favouring sediment instability where erosion and sedimentation processes could be simultaneous.

Spatial integration of τ-values did not reveal any differences between transversal (data not shown) and longitudinal directions (Fig. 5), peaking close to the limit between *C. prolifera* and *C. nodosa.* At 0.03 to 0.04 m over the sediment surface, practically any τ-value exceeded the erosion thresholds. Only for *C. prolifera* on silt environment did some τ range values surpass the erosion threshold. However, erosion conditions are not expected in lower elevations within the canopy, since bottom shear stress usually decreases deeper within the dense canopy of *C. prolifera* (Fig. 6). Therefore, in this particular case, the sediment source is not expected to be local erosion. The probability of sedimentation was clearly low in *C. prolifera*-dominated environments, with the clay fraction having the lowest expected probability of deposition. At HV, most of the transported sediment had no chance to settle on *C. prolifera* beds, but this probability increased at LV mostly for silt and fine sand fractions. In contrast, *C. nodosa*-dominated environments seem to favour the conditions for trapping sediment regardless of particle size or water velocity (Fig. 5). As vertical profiles of Reynold stress under LV conditions had values <0.1 Pa, both canopies can be considered a layer of low τ-values. However, our results also show that *C. nodosa* generates thicker low τ-layers than *C. prolifera* (Fig. 6).

TKE above the canopy

Free stream velocity and bottom microtopography had significant effects on TKE_{above} values in both species (Table 4). Free stream velocity accounted for most of the total variance over the *C. prolifera* canopy (76% compared to 16% attributed to the bottom microtopography), whereas for *C. nodosa*, microtopography explained 36% of the variance (only 28% of the variance was due to free stream velocity). No significant interaction effects between velocity and

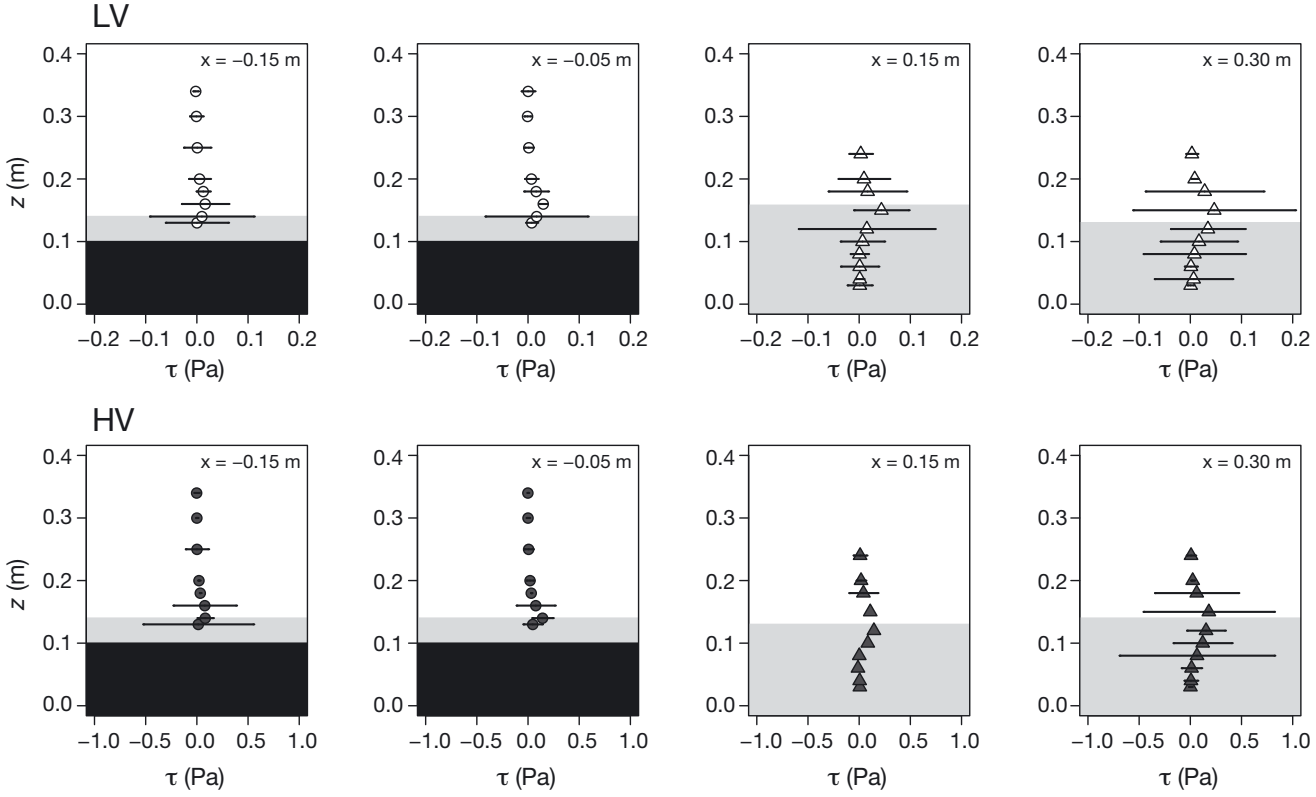

Fig. 6. Comparison of vertical profiles on Reynolds stress (τ) in the stepped bed treatment for *Caulerpa prolifera* (circles) and *Cymodocea nodosa* (triangles), at low velocity (top, white symbols) and high velocity (bottom, dark symbols). The black layer in the *C. prolifera* panels represents the height of the bed. Grey areas represent the canopy. Error bars are 95% CI

Table 4. Statistical effects of free stream velocity and microtopography treatments on turbulent kinetic energy on top of the canopies (TKE_{above}). Level of significance $\alpha = 0.05$; n = 8; SS: sum of squares; MS: mean squares

Factor	df	SS	MS	*F*	% SS	p
(A) *Caulerpa prolifera*						
Free stream velocity	1	8.562	8.562	300.69	76	<0.001
Microtopography	1	1.844	1.844	64.75	16.4	<0.001
Free stream velocity × Microtopography	1	0.068	0.068	2.39	–	0.13
Residuals	28	0.797	0.028			
(B) *Cymodocea nodosa*						
Free stream velocity	1	9.72	9.72	21.90	28	<0.001
Microtopography	1	12.2	12.2	27.49	36	<0.001
Free stream velocity × Microtopography	1	0.016	0.016	0.036	–	0.85
Residuals	28	12.42	0.444			

bottom microtopography were detected for any of the 2 species. Interspecific differences could not be tested due to heteroscedasticity of data even after transformation. However, significant differences were not expected since the 95% confidence intervals for both species overlapped in every treatment (Fig. 7).

DISCUSSION

This study supports our initial hypothesis that flow along stepped TZs results in a gradient of different probabilities of sedimentation for competing macrophyte species. It reinforces the thought of physically mediated interactions at these boundary zones and emphasizes the need for further studies to understand hydrodynamics of transitional bottoms, since they are characteristic of many coastal landscapes.

Hydrodynamics-mediated processes at the TZ

This work reveals that in TZs between overlapping *Caulerpa prolifera* and *Cymodocea nodosa* patches, free stream velocity rather than microtopography dominates turbulence (Tables 3 & 4). This result suggests that in this type of environment, hydrodynamics are more influenced by short-term physical processes (i.e. tides and wind) than by long-term ones (i.e. variables affecting microtopography, Bouma et al. 2007, Borsje et al. 2009). The key role of the free stream velocity in controlling hydrodynamics contrasts with previous reports of TZs for *Spartina maritima* populations. For this saltmarsh plant, bed elevation (related to sediment accretion and, therefore, a long-term process) was considered to be the major factor determining exposure to tidal currents (Castellanos et al. 1994, Sanchez et al. 2001). The control by short-term processes implies that those with high temporal heterogeneity dominate changes at these boundary zones, which is the common situation in intertidal areas. Hence, the role of microtopography cannot be regarded as a mechanism independent from flow velocity (Fonseca et al. 1983).

In our experiments, the enhancement of unidirectional currents (from 0.06 to 0.14 m s^{-1}) co-occurred with increases in turbulence, including (1) TKE_{above} and (2) bottom shear stress. In a situation where the sediment concentration in the water column is high, the rise in TKE_{above} (2.5-fold for both species) suggests the augmentation in vertical sediment transport from the overlaying flow (Nepf et al. 2007, Hendriks et al. 2010). However, increases in bottom shear stress were not necessarily related to decreases in probability for sedimentation, since sedimentation is strongly dependent on particle size-specific τ_{sed} thresholds (Zong & Nepf 2010). Within the velocity range used in our experiment, *C. nodosa* did seem to always favour sediment deposition (i.e. free stream velocity had no significant effects), whereas in *C. prolifera* canopies, the effects seem to depend on the combination of free stream velocity and grain size (Fig. 5). *C. prolifera* did appear to facilitate sediment deposi-

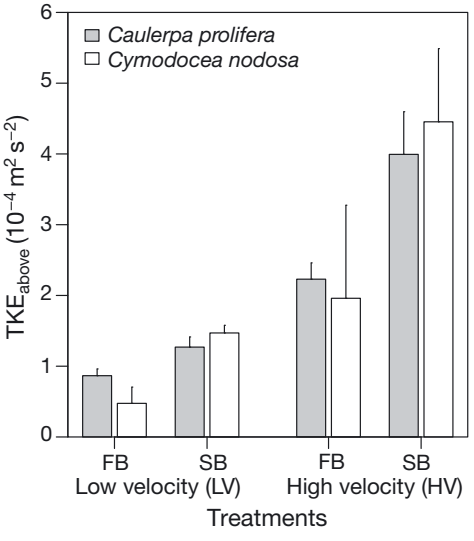

Fig. 7. Turbulent kinetic energy (TKE_{above}) over canopies of *Caulerpa prolifera* and *Cymodocea nodosa* according to the experimental treatments (FB: flat bottom; SB: stepped bottom). Error bars correspond to +95% confidence intervals

tion only for silt and fine-sand fractions under LV conditions; however, at HV, although it does not favour erosion, it seemed to favour conditions for sediment suspension more than for deposition. Therefore, species-specific differences on sedimentation probability are only expected under HV scenarios.

Our experiment simulated values of unidirectional currents expected at CBNP under strong wind conditions (HV; Alvarez et al. 1999, Kagan et al. 2003). Under this scenario, sediment remobilization is expected. However, our results showed that the intensity of unidirectional currents generated under these conditions was not high enough to foster the risk of erosion, highlighting the importance of waves even in environments protected from oceanic waves, such as CBNP (Amos et al. 2004). Waves enhance shear stress levels, which may control the structure of seagrass beds in shallow embayments (Carr et al. 2016). Additionally, the erosion threshold can be increased by sediment-stabilizers like microphytobenthos (Amos et al. 2004) or decreased by sediment-destabilizers like bioturbators (Widdows & Brinsley 2002). Hence, further *in situ* studies are needed for a better understanding of sediment dynamics on vegetated foreshores, particularly during wind-wave dominated events.

Besides bottom stability, particle retention within submersed canopies can also be related to horizontal sediment transport (Gacia et al. 1999, Peralta et al. 2008). Considering the canopy volumetric flow rate ($\%Q_c$) as a proxy for the source of particles, our results support previous findings that highlighted the dependency of volumetric flow rate the on species-specific canopy height and permeability (Fig. 4) (Morris et al. 2013). *C. prolifera* stands are denser and shorter, exhibiting a low permeability ($\%Q_c$ = 1.5–3.5%). Therefore, the main source of particles must be the vertical transport driven by turbulent mixing. In contrast, *C. nodosa* beds are sparser and highly permeable ($\%Q_c$ = 3.5–8%), suggesting that the main source of particles must be provided by horizontal transport (advection, Hendriks et al. 2010). Under these conditions, the preferential pathway of sediments from upstream towards *C. nodosa* beds seems a reasonable scenario.

Microtopography can also affect sediment transport. The existence of small-scale microtopography on vegetated bottoms (i.e. 0.1 m; Fonseca et al. 1983, Carpenter & Williams 1993) has previously been associated with generation of LV areas. In our case, the SB favoured the generation of a LV layer in the depressed areas of *C. nodosa* (Fig. 3), probably fostering a depositional environment (Hendriks et al. 2010). However, SB probably also reduces sediment availability (e.g. Q_c decreases with decreasing velocity, Fig. 4), as an indirect consequence of reducing velocity. Therefore, the efficiency of beds thriving on SBs as sediment traps seems to be restricted to events that promote high sediment loads in the water column (e.g. after a storm; Koch 1999).

Consequences for experimentation in benthic TZs

Previous flume-tank studies on single-species patches suggest that turbulence patterns strongly depended on bed configuration. For example, large homogeneous canopies produced a stronger dissipation of turbulent wakes than small and scattered patches did (Folkard 2005, Maltese et al. 2007). Similar effects were observed in the field (Lara et al. 2012), indicating that the design of appropriate experimental spatial set-ups is key to obtaining flume-tank results that are scalable to real landscapes (Fonseca & Koehl 2006). Consequently, setting up a homogeneous bed within a flume tank is not useful to understand processes occurring in patchy landscapes. Moreover, our results suggest that spatial variability in τ and TKE_{above} was better explained by the transition between 2 vegetation types; this was supported by previous *in situ* measurements (Morris et al. 2013). The success of experiments involving patchy configurations, either monospecific or multispecific, reveals that such approaches may be promising for future research (Bal et al. 2013, Bouma et al. 2013).

Our study suggests that both hydrodynamic and sedimentary processes occurring in TZs between *C. prolifera* and *C. nodosa* patches may play an important role in interspecific competition for space. Differences in their bathymetric distribution can be explained by differences in light requirements. However, smooth-sloped subtidal habitats are areas where the corresponding niches overlap and competition must occur (Terrados & Ros 1991). Despite previous research, pinpointing processes controlling shallow subtidal competition still remains difficult (Pérez-Ruzafa et al. 2012). This work identifies, at the patch scale, the physical processes that could be involved, suggesting that *C. nodosa* patches are more likely to be depositional areas in TZs when occurring adjacent to *C. prolifera* patches. This depositional scenario would favour a successful outcome for *C. prolifera* when competing for space, because (1) *C. nodosa* is highly sensitive to burial and siltation (Ceccherelli & Campo 2002), especially under similar

heights used for our SB level (>0.07 m, Marbà & Duarte 1994, Tuya et al. 2013b); and because (2) *C. prolifera* has higher biomass turnover and horizontal elongation rates than *C. nodosa* (Brun et al. 2006, Vergara et al. 2012), favouring a rapid spread even at short time scales.

In conclusion, the role of bottom microtopography is supported as a flow-structuring factor in TZs between patches of structurally contrasting macrophyte species. Nevertheless, together with microtopography, the free stream velocity must also be taken into account, because of its major role in controlling sediment stability. In the particular case of Cádiz Bay under scenarios of no wave generation (e.g. no wind or no fetch conditions), high unidirectional currents (~0.14 m s^{-1}) may increase the probability of sedimentation in *C. nodosa* patch edges more than in *C. prolifera*. These features are key to define the hydrodynamic environment in transition areas between these 2 macrophyte species, both of which are considered ecosystem engineers for sediment dynamics in shallow and protected subtidal habitats.

Acknowledgements. This work was supported by the Spanish National Research Projects EVAMARIA (CTM2005-00395/MAR) and IMACHYDRO (CTM2008-0012/MAR) and by the Andalusian Excellence Research Project FUNDIV P07-RNM-02516. M.L. was supported by an FPI grant of the Spanish Ministry of Science and Technology and a bridge contract of the University of Cádiz. M.L. especially thanks Thijs and other anonymous PhD students for their valuable help in collecting sediments. NIOZ is gratefully acknowledged for granting access to the flume facilities at NIOZ-Yerseke to carry out these experiments. This is CEIMAR Journal publication no. 137.

LITERATURE CITED

Achab M, Gutierrez-Mas JM (2005) Nature and distribution of the sand fraction components in the Cadiz Bay bottoms (SW-Spain). Rev Soc Geol Esp 18:133–143

Almasi MN, Hoskin CM, Reed JK, Milo J (1987) Effects of natural and artificial *Thalassia* on rates of sedimentation. J Sediment Petrol 57:901–906

Alvarez O, Izquierdo A, Tejedor B, Mañanes R, Tejedor L, Kagan BA (1999) The influence of sediment load on tidal dynamics, a case study: Cádiz Bay. Estuar Coast Shelf Sci 48:439–450

Alvarez O, Tejedor B, Tejedor L, Kagan BA (2003) A note on sea-breeze-induced seasonal variability in the K1 tidal constants in Cádiz Bay, Spain. Estuar Coast Shelf Sci 58: 805–812

Amos CL, Bergamasco A, Umgiesser G, Cappurci S and others (2004) The stability of tidal flats in Venice Lagoon — the results of *in-situ* measurements using two benthic, annular flumes. J Mar Syst 51:211–241

Bal KD, Brion N, Woulé-Ebongué V, Schoelynck J and others (2013) Influence of hydraulics on the uptake of ammonium by two freshwater plants. Freshw Biol 58: 2452–2463

Borsje BW, de Vries MB, Bouma TJ, Besio G, Hulscher SJMH, Herman PMJ (2009) Modelling bio-geomorphological influences for offshore sandwaves. Cont Shelf Res 29:1289–1301

Bouma TJ, van Duren LA, Temmerman S, Claverie T, Blanco-Garcia A, Ysebaert T, Herman PMJ (2007) Spatial flow and sedimentation patterns within patches of epibenthic structures: combining field, flume and modelling experiments. Cont Shelf Res 27:1020–1045

Bouma TJ, Temmerman S, van Duren LA, Martini E and others (2013) Organism traits determine the strength of scale-dependent bio-geomorphic feedbacks: a flume study on three intertidal plant species. Geomorphology 180-181:57–65

Brun FG, Vergara JJ, Peralta G, García Sánchez MP, Hernández I, Pérez-Lloréns JL (2006) Clonal building, simple growth rules and phylloclimate as key steps to develop functional–structural seagrass models. Mar Ecol Prog Ser 323:133–148

Bulleri F, Balata D, Bertocci I, Tamburello L, Benedetti-Cecchi L (2010) The seaweed *Caulerpa racemosa* on Mediterranean rocky reefs: from passenger to driver of ecological change. Ecology 91:2205–2212

Carpenter RC, Williams SL (1993) Effects of algal turf canopy height and microscale substratum topography on profiles of flow speed in a coral forereef environment. Limnol Oceanogr 38:687–694

Carr JA, D'Odorico P, McGlathery KJ, Wiberg PL (2016) Spatially explicit feedbacks between seagrass meadow structure, sediment and light: habitat suitability for seagrass growth. Adv Water Resour 93:315–325

Castellanos EM, Figueroa ME, Davy AJ (1994) Nucleation and facilitation in saltmarsh succession: interactions between *Spartina maritima* and *Athrocnemum perenne*. J Ecol 82:239–248

Ceccherelli G, Campo D (2002) Different effects of *Caulerpa racemosa* on two co-occurring seagrasses in the Mediterranean. Bot Mar 45:71–76

Ceccherelli G, Cinelli F (1999) Effects of *Posidonia oceanica* canopy on *Caulerpa taxifolia* size in a north-western Mediterranean bay. J Exp Mar Biol Ecol 240:19–36

Chang TS, Flemming BW (2013) Ripples in intertidal mud — a conceptual explanation. Geo-Mar Lett 33:449–461

Dade WB, Hogg AJ, Boudreau BP (2001) Physics of flow above the sediment water interface. In: Boudreau BP, Jorgensen BB (eds) The benthic boundary layer: transport processes and biogeochemistry. Oxford University Press, New York, NY, p 23–27

De los Santos CB, Brun FG, Vergara JJ, Pérez-Lloréns JL (2013) New aspect in seagrass acclimation: leaf mechanical properties vary spatially and seasonally in the temperate species *Cymodocea nodosa* Ucria (Ascherson). Mar Biol 160:1083–1093

Folkard AM (2005) Hydrodynamics of model *Posidonia oceanica* patches in shallow water. Limnol Oceanogr 50: 1592–1600

Fonseca MS, Fischer JS (1986) A comparison of canopy friction and sediment movement between four species of seagrass with reference to their ecology and restoration. Mar Ecol Prog Ser 29:15–22

Fonseca MS, Koehl MAR (2006) Flow in seagrass canopies: the influence of patch width. Estuar Coast Shelf Sci 67: 1–9

Fonseca MS, Zieman JC, Thayer GW, Fisher JS (1983) The role of current velocity in structuring eelgrass (*Zostera marina* L.) meadows. Estuar Coast Shelf Sci 17:367–380

Gacia E, Granata T, Duarte CM (1999) An approach to the measurement of particle flux and sediment retention within seagrass (*Posidonia oceanica*) meadows. Aquat Bot 65:255–268

Gacia E, Duarte CM, Marbà N, Terrados J, Keneddy H, Fortes MD, Tri NH (2003) Sediment deposition and production in SE-Asia seagrass meadows. Estuar Coast Shelf Sci 56:909–919

Gutierrez-Mas JM, Lopez-Galindo A, Lopez-Aguayo F (1997) Clay minerals in recent sediments of the continental shelf and the Bay of Cádiz (SW, Spain). Clay Miner 32: 507–515

Hendriks IE, Bouma TJ, Morris EP, Duarte CM (2010) Effects of seagrass and algae of the *Caulerpa* family on hydrodynamics and particle trapping rates. Mar Biol 157: 473–481

Hoffman R (2014) Alien benthic algae and seagrasses in the Mediterranean Sea and their connection to global warming. In: Goffredo S, Dubinsky Z (eds) The Mediterranean Sea. Its history and present challenges. Springer-Science+Business Media, Dordrecht, p 159–181

Holmer M, Marbà N, Lamote M, Duarte CM (2009) Deterioration of sediment quality in seagrass meadows (*Posidonia oceanica*) invaded by macroalgae (*Caulerpa* sp.). Estuaries Coasts 32:456–466

Irving AD, Connell SD (2002) Interactive effects of sedimentation and microtopography on the abundance of subtidal turf-forming algae. Phycologia 41:517–522

Jonsson PR, Van Duren LA, Amielh M, Asmus R and others (2006) Making water flow: a comparison of the hydrodynamic characteristics of 12 different benthic biological flumes. Aquat Ecol 40:409–438

Kagan BA, Alvarez O, Izquierdo A, Mañanes R, Tejedor B, Tejedor L (2003) Weak wind-wave/tide interaction over a moveable bottom: results of numerical experiments in Cadiz Bay. Cont Shelf Res 23:435–456

Koch EW (1999) Sediment resuspension in a shallow *Thalassia testudinum* Banks ex König bed. Aquat Bot 65:269–280

Lara M, Peralta G, Alonso JJ, Morris EP, González-Ortiz V, Rueda-Márquez JJ, Pérez-Lloréns JL (2012) Effects of intertidal seagrass habitat fragmentation on turbulent diffusion and retention time of solutes. Mar Pollut Bull 64:2471–2479

Maltese A, Cox E, Folkard A, Ciraolo G, La Loggia G, Lombardo G (2007) Laboratory measurements of flow and turbulence in discontinuous distributions of ligulate seagrass. J Hydraul Eng 133:750–760

Marani M, Lanzoni S, Silvestri S, Rinaldo A (2004) Tidal landforms, patterns of halophytic vegetation and the fate of the lagoon of Venice. J Mar Syst 51:191–210

Marbà N, Duarte CM (1994) Growth response of the seagrass *Cymodocea nodosa* to burial and erosion. Mar Ecol Prog Ser 107:307–311

Morris EP, Peralta G, Benavente J, Freitas R and others (2009) *Caulerpa prolifera* stable isotope ratios reveal anthropogenic nutrients within a tidal lagoon. Mar Ecol Prog Ser 390:117–128

Morris EP, Peralta G, Van Engeland T, Bouma TJ and others (2013) The role of hydrodynamics in structuring in situ ammonium uptake within a submerged macrophyte community. Limnol Oceanogr Fluids Environ 3:210–224

Nepf H, Ghisalberti M, White B, Murphy E (2007) Retention time and dispersion associated with submerged aquatic canopies. Water Resour Res 43:W04422

Occhipinti-Ambrogi A, Savini D (2003) Biological invasions as a component of global change in stressed marine ecosystems. Mar Pollut Bull 46:542–551

Olivé I, Vergara JJ, Pérez-Lloréns JL (2013) Photosynthetic and morphological photoacclimation of the seagrass *Cymodocea nodosa* to season, depth and leaf position. Mar Biol 160:285–297

Orth RJ, Carruthers TJB, Dennison WC, Duarte CM and others (2006) A global crisis for seagrass ecosystems. Bioscience 56:987–996

Peralta G, van Duren LA, Morris EP, Bouma TJ (2008) Consequences of shoot density and stiffness for ecosystem engineering by benthic macrophytes in flow dominated areas: a hydrodynamic flume study. Mar Ecol Prog Ser 368:103–115

Pérez M, Romero J (1992) Photosynthetic response to light and temperature of the seagrass *Cymodocea nodosa* and the prediction of its seasonality. Aquat Bot 43:51–62

Pérez-Lloréns JL, Vergara JJ, Olivé I, Mercado JM, Conde-Álvarez R, Pérez-Ruzafa A, Figueroa FL (2014) Autochthonous seagrasses. In: Goffredo S, Dubinsky Z (eds) The Mediterranean Sea. Its history and present challenges. Springer-Science+Business Media, Dordrecht, p 137–158

Pérez-Ruzafa A, Marcos C, Bernal CM, Quintino V and others (2012) *Cymodocea nodosa* vs *Caulerpa prolifera*: causes and consequences of a long term history of interaction in macrophyte meadows in the Mar Menor coastal lagoon (Spain, southwestern Mediterranean). Estuar Coast Shelf Sci 110:101–115

Piazzi L, Balata D, Ceccherelli G, Cinelli F (2005) Interactive effect of sedimentation and *Caulerpa racemosa* var. *cylindracea* invasion on macroalgal assemblages in the Mediterranean Sea. Estuar Coast Shelf Sci 64:467–474

Piazzi L, Balata D, Foresi L, Cristaudo C, Cinelli F (2007) Sediment as a constituent of Mediterranean benthic communities dominated by *Caulerpa racemosa* var. *cylindracea.* Sci Mar 71:129–135

Sanchez JM, San Leon DG, Izco J (2001) Primary colonisation of mudflat estuaries by *Spartina maritima* (Curtis) Fernald in northwest Spain: vegetation structure and sediment accretion. Aquat Bot 69:15–25

Self RFL, Nowell ARM, Jumars PA (1989) Factors controlling critical shears for deposition and erosion of individual grains. Mar Geol 86:181–199

Smith C, Walters LJ (1999) Fragmentation as a strategy for *Caulerpa* species: fates of fragments and implications for management of an invasive weed. Mar Ecol 20:307–319

Sokal RR, Rohlf FJ (1995) Biometry. The principles and practice of statistics in biological research, 3rd edn. WH Freeman and Company, New York, NY

Stafford NB, Bell SS (2006) Space competition between seagrass and *Caulerpa prolifera* (Forsskaal) Lamouroux following simulated disturbances in Lassing Park, FL. J Exp Mar Biol Ecol 333:49–57

Terrados J, Ros JD (1991) Production dynamics in a macrophyte-dominated ecosystem: the Mar Menor coastal lagoon (SE Spain). Oecol Aquat 10:255–270

Tuya F, Hernandez-Zerpa H, Espino F, Haroun R (2013a) Drastic decadal decline of the seagrass *Cymodocea nodosa* at Gran Canaria (eastern Atlantic): interactions with the green algae *Caulerpa prolifera.* Aquat Bot 105: 1–6

Tuya F, Espino F, Terrados J (2013b) Preservation of seagrass clonal integration buffers against burial stress. J Exp Mar Biol Ecol 439:42–46

van Rijn LC (2007) Unified view of sediment transport by currents and waves. I: Initiation of motion, bed roughness and bed-load transport. J Hydraul Eng 133: 649–667

Vergara JJ, García-Sánchez MP, Olivé I, García-Marín P, Brun FG, Pérez-Lloréns JL, Hernández I (2012) Seasonal functioning and dynamics of *Caulerpa prolifera* meadows in shallow areas: an integrated approach in Cadiz Bay Natural Park. Estuar Coast Shelf Sci 112:255–264

Whitehouse RJS, Bassoullet P, Dyer KR, Mitchener HJ, Roberts W (2000) The influence of bedforms on flow and sediment transport over intertidal mudflats. Cont Shelf Res 20:1099–1124

Widdows J, Brinsley M (2002) Impact of biotic and abiotic processes on sediment dynamics and the consequences to the structure and functioning of the intertidal zone. J Sea Res 48:143–156

Williams SL (2007) Introduced species in seagrass ecosystems: status and concerns. J Exp Mar Biol Ecol 350: 89–110

Wright JT, Davis AR (2006) Demographic feedback between clonal growth and fragmentation in an invasive seaweed. Ecology 87:1744–1754

Zong L, Nepf H (2010) Flow and deposition in and around a finite patch of vegetation. Geomorphology 116:363–372

Editorial responsibility: Kenneth Heck Jr, Dauphin Island, Alabama, USA

Submitted: March 8, 2016; Accepted: September 27, 2016
Proofs received from author(s): December 7, 2016